

DISCLAIMER

This report was prepared as an account of work sponsored by an agency of the United States Government. Neither the United States Government nor any agency thereof, nor any of their employees, makes any warranty, express or implied, or assumes any legal liability or responsibility for the accuracy, completeness, or usefulness of any information, apparatus, product, or process disclosed, or represents that its use would not infringe privately owned rights. Reference herein to any specific commercial product, process, or service by trade name, trademark, manufacturer, or otherwise does not necessarily constitute or imply its endorsement, recommendation, or favoring by the United States Government or any agency thereof. The views and opinions of authors expressed herein do not necessarily state or reflect those of the United States Government or any agency thereof.

This report has been reproduced directly from the best available copy.

Available to DOE and DOE contractors from the Office of Scientific and Technical Information, P.O. Box 62, Oak Ridge, TN 37831; prices available from (615)576-8401, FTS 626-8401.

Available to the public from the National Technical Information Service, U.S. Department of Commerce, 5285 Port Royal Rd., Springfield, VA 22161.

Visualization of Foam/Oil in a New, High Resolution, Sandstone
Replica Micromodel

SUPRI TR 86

By
John Wirt Hornbrook
Paul Pettit
Louis M. Castanier

August 1992

Work Performed Under Contract No. DE-FG22-90BC14600

Prepared for
U.S. Department of Energy
Assistant Secretary for Fossil Energy

Thomas B. Reid, Project Manager
Bartlesville Project Office
P. O. Box 1398
Bartlesville, OK 74005

Prepared by
Stanford University
Petroleum Research Institute
Stanford, CA 94305

Abstract

A new micromodel construction procedure has been developed as a tool to better understand and model pore level events in porous media. The construction procedure allows for the almost exact two-dimensional replication of any porous medium of interest. For the case presented here, a Berea sandstone was chosen.

Starting with a thin section of the porous medium of interest, a two-dimensional replica of the flow path is etched into a silicon wafer to a prescribed depth. Bonding the etched pattern to a flat glass plate isolates the flow path and allows the pore level flow events to be studied.

The high resolution micromodels constructed with the new procedure were used to study the effects of oil on the displacement characteristics of foam in a porous medium of intermediate wettability. A crude oil was injected into the micromodel, partially filling it. The oil was then produced under two different displacement schemes. First, a slug of surfactant was used. Second, foam generated in situ, far from the oil bank, was used to displace the oil.

Qualitative observations indicate significant differences at the interface between the oil and the displacing phase. When slug surfactant injection is used, the oil appears to wet the surface. The oil displacement process is efficient due to a large fractional production of oil from the large pores before the surfactant breaks through. When in-situ foam is the displacing phase, the foam is observed to break near the oil interface. The liquid phase in the foam becomes the wetting phase. It is observed to reside in the small pores and to coat most of the grain surfaces. Displacement of oil under this injection scheme is inefficient due to transfer of the surfactant along grain edges and subsequent early breakthrough of the surfactant.

Contents

Acknowledgements	ii
Abstract	iii
List of Figures	v
1 Introduction	1
2 Literature Review	2
3 Micromodel Construction	4
3.1 Photographic procedure	4
3.2 Computer manipulation	5
3.3 Image transfer and etching	5
3.4 Anodic bonding	6
3.5 Final construction	7
4 Experimental Equipment	15
5 Experimental Procedure	17
5.1 Experimental procedure	17
5.2 Slug surfactant displacement of oil	17
5.3 Foam displacement of oil	17
6 Conclusions	23
7 Recommendations	24
A Computer Program	25
References	30

List of Figures

3.1	Schematic of micromodel construction procedure	8
3.2	Example of digital manipulation	9
3.3	Image mask schematic	10
3.4	Image transfer schematic	11
3.5	Initial and final equilibrium DC potential distributions across the corning glass during anodic bonding. (After Terry)	12
3.6	Anodic bonding of glass and silicon	13
3.7	Top and side views of completed micromodel	14
4.1	Experimental apparatus schematic	16
5.1	Crude oil/slug-surfactant interface	19
5.2	Bulk foam near injection port - far from oil bank	20
5.3	High quality foam in porous medium	21
5.4	Crude oil/foam interface	22

1. Introduction

Since the late 1950's foam has been recognized as a fluid possessing oil production enhancement capability. Foam may be used to improve the mobility characteristics of an oil reservoir or it may be used as a selective blocking agent to reduce the effects of fingering induced by permeability streaks in the producing formation. Additionally, the surfactants used to produce foams may aid in the production of heavy oils by partially dissolving the oil or by helping to separate oil blobs from the rock in mixed-wet systems.

There are essentially three levels of investigation at which the flow of foam in porous media may be studied – field level, core level, and pore level. The field level is the coarsest level and provides researchers with, usually, field specific information about the characteristics of foam flow in porous media. Naturally, since all observations are indirect, conclusions about foam flow drawn from field level experiments do not usually focus on the fundamentals of foam flow and are usually not applicable in a general sense.

Core level experiments are usually attempts to obtain more general results from foam flow experiments. In core floods, the experimenter is better able to understand the underlying mechanisms of foam flow in porous media due to better control of boundary conditions and greater ease in observation. However, the experimenter is still unable to directly observe the flow of foam. For direct observation of foam, micromodels were developed.

Micromodels represent the smallest scale (the pore scale) for the study of foam flow in porous media (or any flow for that matter). By directly observing how foam flows through a porous medium, the experimenter is able to understand underlying mechanisms and, in conjunction with larger scale experiments, is better able to model the effects of foam floods. The biggest problem with micromodels is that they may not accurately represent an actual porous medium. Several types of micromodels have been used in the past all of which have severe shortcomings that limit their usefulness as an investigative tool.

The most commonly used micromodels are bead pack, slab, etched glass, and etched silicon micromodels. All of the micromodels listed above have problems inherent in the construction procedure except for the silicon micromodels. (A detailed review of the shortcomings are found in the literature review section of this paper.) Silicon micromodels are especially useful because they may be etched precisely at a very small scale. This characteristic of silicon has not been taken advantage of in the past, however. It was the focus of this research to take advantage of the precision etching characteristic of silicon to replicate, in two dimensions, a porous medium. After construction of this new high resolution micromodel, the effects of crude oil on the displacement characteristics of foam were observed.

2. Literature Review

The study of foam with application to petroleum engineering began with the pioneering work of Bond and Holbrook[1] in 1958. Their work concentrated on the mobility effects of injected foam and it pointed out the benefits to foam injection as a method of enhancing oil reservoir performance. Over the next thirty years much research and several field experiments have attempted to understand the flow of foam in porous media on both a qualitative and quantitative level.

Many papers have been written on the fluid properties of foam. The results of these papers are rarely in agreement on the nature of foam and are often contradictory. Two chronological reviews of foam research have been carried out; by Marsden et. al.[7] and Marsden[6] in 1977 and 1986, respectively. In his reviews, Marsden outlines the major advances in the understanding of foam flow and points out shortcomings and contradictions in existing work. A brief summary of foam fluid properties from Marsden is:

1. Foam is a fluid of high apparent viscosity.
2. Foam viscosity is a function of the surfactant concentration.
3. Foam viscosity is a function of flow rate.
4. The flow history of foam affects its viscosity.

Foam flow mechanisms, the means by which foam propagates through a porous medium, have been studied in numerous papers as well. Most of this work, however, has focused on a qualitative description of foam rather than a quantitative one. Most recently, the research of Owete[9] (1984), and Jimenez and Radke[4] (1988) have attempted to extend the understanding of foam flow mechanisms beyond the description of observed phenomena. Owete studied the flow of foam in the following two areas:

1. The propagation of foam and its components.
2. The mobility of gas in the presence of foam.

Owete carried out his work in micromodels with homogeneous and heterogeneous flow paths and, although most of his conclusions are qualitative, some quantitative results were obtained. Owete observed that foam may propagate both as a bulk fluid and also as two distinct phases as lamellae break and reform. These observations have been verified by several other researchers since Owete.

Owete's results for a homogeneous micromodel have been verified as a part of the background work in my research. The qualitative aspects of Owete's work have been extended to include the effects of foam injection procedure on oil displacement. Unlike Owete's research, however, the current research was carried out in a two-dimensional replica of a Berea sandstone with pore sizes the same as those in real porous media.

Research on the effects of oil on foam has been carried out by Nikolov et. al.[8], Manlowe and Radke[5] (1988), and Sanchez and Hazlett[10] (1989). Nikolov et. al. studied foam stability in the presence of a crude oil with various surfactants. They point out the complexities in foam destabilization by oil and offer several criteria for selecting a stable foam-forming surfactant. Manlowe and Radke studied the foam breaking tendency of oil and described the stability of a pseudo-emulsion film as the determinant of foam stability in the presence of oil. Sanchez and Hazlett found that foam forms in oil-wet porous media by altering the surface characteristics of the flow path. The results of Sanchez and Hazlett provide important insight into the results of this

report. Research described in this report investigates the stability of the oil/displacement phase interface under two foam injection schemes. Background for this specific area of foam flow study is provided by Hutchinson[3] who describes the work of Stanford researchers. They found that in the displacement of oil, the foam injection procedure plays a significant role. When a slug of surfactant was injected prior to foam injection, a stable front developed and an efficient oil displacement was achieved. When externally generated foam was used to displace the oil, however, a stable front could not be achieved and surfactant quickly channeled through the oil. The research described in this report provides a possible explanation for these phenomena.

Research involving flow of foam through micromodels is relatively new. In addition to the micromodel research mentioned above (references 4 through 6), several studies on the usefulness of micromodels as a research tool have been carried out. Sarathi[11] (1986) studied several types of micromodels to determine their strengths and weaknesses as research tools. He concludes that micromodels can yield advantages in studying pore level events but warns against extrapolating pore level events to a large scale without additional information. He also lists several disadvantages inherent in commonly used micromodels, most of which will be eliminated by the construction process outlined in this report. Sarathi cites the following as important problems with micromodel research:

1. Difficulty in obtaining a continuous specific etch depth.
2. Introduction of microscopic heterogeneity into the model in the etch procedure.
3. Difficulty in replicating reservoir Peclet number due to enlargement of the pores.
4. Loss of three-dimensional continuity.
5. Loss of detail - in heterogeneity, pore geometry, connectivity, and surface roughness - due to the annealing process used in most micromodel construction processes.

Except for the loss of three dimensional continuity, all of the disadvantages listed above are eliminated in the micromodels described in this report.

Huh et. al.[2] (1989) studied the effects of differences in heterogeneity on foam generation in porous media. Their research indicates that heterogeneity plays a very important role in determining the propagation characteristics of foam in porous media. This result indicates that a micromodel must replicate a porous medium of interest as closely as possible in order to be a useful tool for study of foam in that porous medium.

3. Micromodel Construction

Micromodel construction is carried out in a five step procedure that results in the detailed replication and isolation of a flow path of interest. The five step procedure (Fig.3.1) consists of photography, computer manipulation, image transfer and etching, anodic bonding, and final construction.

3.1 Photographic procedure

As the starting point in the flow path construction procedure, a suitable flow path must be selected. This may be any real or man-made flow path. The sample used in this study was a clean Berea sandstone.

First, construct a thin section of the berea sample using blue epoxy to fill all void spaces (A blue or yellow coloring is preferred to simplify photographic procedures which will be described later). Preparation of thin sections results, visually, in the reduction of the three-dimensional flow space to a two-dimensional approximation. As a result, some continuous pores are made discontinuous while some new, continuous flow paths are created. By changing the focal length of the microscope, it is possible to discover the pore configuration before the creation of a thin section. Microscopic analysis was used on the berea sample and a section approximately two and one-half centimeters long by one and one-half centimeters high was selected as most closely approximating the three-dimensional pore system in the berea sample.

A color slide photograph was taken of the selected flow path rectangle. In the photograph, the pore spaces appeared blue while the rock grains appeared black. Professional color slide film was used to photograph the image to assure high quality results. Professional film guarantees that the film itself will not impair results and the use of color film reduces the influence of light levels and exposure time on image quality. Once a high quality color image has been made of the flow path the process of transforming it into a black and white image begins. All black and white image work for the berea sample was carried out by a professional black and white lab.

A black and white negative is made of the color slide of the flow path. In the process of changing from color to black and white, light blues and light yellows are not recognized, so these areas are recorded as white. The use of clear epoxy should be avoided in the construction of the thin section because, with no dark colors present, light refraction becomes a problem and high quality images are difficult to obtain. Black epoxy should be avoided for the obvious reason that the entire sample will appear black on film, and epoxies dyed with red dyes should be avoided for the same reason. In the transference of the image from color film to black and white film, reds and sometimes oranges appear black.

After successful transference of the color image to black and white, the flow path image will exist as a gray scale negative. The remaining step in image preparation is to eliminate gray scales to produce a true black and white image. This is accomplished by first reversing the gray scale negative and then creating a line art copy of the positive. A line art copy is basically a specialized photocopy of a black and white image in which gray scale thresholding is used to define absolute black and white. The line art copy is then printed on a slide.

At the conclusion of the photographic process, an exact black and white image of the selected flow path has been produced. Now, further manipulation of the image is necessary.

3.2 Computer manipulation

After obtaining a black and white slide of the flow path, the image was transferred to TIFF format by use of a high resolution scanner. The scanning was carried out by Pacific Digital, Inc. An approximately square section of the slide was selected for ease in manipulation (approximately 1.5 cm by 1.5 cm) and the image was scanned at 870 pixels per inch. The resulting image was then 512 pixels high by 512 pixels wide. The image, now in TIFF format, was then analyzed on a Macintosh computer by using IMAGE, a digital image analysis package, to determine if a realistic, continuous flow path had been captured. While the image was, indeed, a very realistic image of an actual flow path, it was found that there were no continuous flow paths through the image. By use of tools available in IMAGE, the necessary pixels were removed to obtain a continuous flow path. The resulting TIFF image fulfilled the necessary requirements - realistic flow path, and a continuous flow path (Fig.3.2). In this, the scanning and manipulation step, the resolution and nature of the flow path can be easily altered. By scanning at a lower resolution, a rougher, more approximate image is obtained, while scanning at a higher resolution results in a smoother, more realistic image. It was felt that the resolution used was high enough for a realistic flow path replication. Manipulation must be done carefully to avoid destroying the flow path characteristics. The main purpose of this report is to develop a procedure for constructing high resolution, accurate replicas of natural flow paths. Meddling with the flow path should be avoided if at all possible. The next step determines the absolute size of the flow path.

In the next step, the TIFF image is transformed into a file that can be read by Stanford's MEBES machine. The TIFF file is converted to a cif file by a program developed at Lawrence Livermore Laboratories (the program is included in Appendix A). In the cif file, the size of pixels are specified. These can range anywhere from 0.25 microns to several microns. By selection of the pixel size, the absolute sizes of the various features of the micromodel can be chosen to replicate, exactly, the corresponding features in the original flow path sample. In cif format the image is broken into a series of rectangles of equivalent pixel value (i.e. white pixels are stored with white pixels and black with black) and these larger rectangles are stored based on location. Once the image is stored in cif format, it is sent to the MEBES machine where it is reformatted once again. This time, it is read a long, narrow rectangles and the file is then stored to be used to create a mask. In transference to MEBES format, the original flow path was replicated 100 times and formed into the smallest repeated MEBES unit - a 10 by 10 grid of the original flow path. When the mask was constructed, the smallest MEBES unit was, again, replicated 100 times and a 10 by 10 grid of the MEBES unit was used to create the image mask. A schematic of the image mask (Fig.3.3) shows the pattern used.

In the construction of the image mask, care was taken to assure continuation of the flow path at the interfaces between the replicated flow path images. To assure continuity in the flow paths, the extreme edges of the flow path image were slightly altered to assure that connection of the replicated images in any arrangement would result in a continuous flow path.

3.3 Image transfer and etching

After computer manipulation, the flow path image is reproduced as a chrome on glass replica of the original flow path at any prescribed magnification. For obvious reasons, a 1:1 replication of the flow path was used. On the mask, grains are opaque while pores are transparent. Transference of the image from the mask to the silicon wafer is carried out by use of a photoresist material.

A coating of the photoresist is spun onto the wafer and, when dry, the wafer is placed into direct contact with the image mask. Ultraviolet light is shined through the image mask. The ultraviolet light kills the photoresist upon contact, so after exposure, the flow path image exists

upon the silicon wafer with grains consisting of photoresist material and pores consisting of clean silicon (Fig.3.4).

After image transfer, the image is etched by a dry etch technique. All areas that are not covered by the photoresist are etched. During the etch, the photoresist is slowly destroyed, so the etch depth of the pores is a function of the thickness of the photoresist delineating the grains. Unfortunately, building a very thick photoresist layer to allow a deep etch may cause loss of detail on the grain surfaces. Also, a very deep etch may cause undercut in the walls which may result in poor isolation of the pores in the bonding step. Great care must be taken to assure that the proper etch depth is obtained without creating other problems in the micromodel construction. The models used in this research were etched to a depth of 5 microns to assure that no grain detail was lost but it should be possible to etch to a depth of 20 to 30 microns with pore throats of 1 micron without any loss of detail.

3.4 Anodic bonding

After constructing the flow model, as described above, it was necessary to isolate the individual etched flow channels in order to observe the flow of foam in isolated pores. The most efficient means to isolate the flow channels was determined to be the bonding of the etched wafer to a flat piece of glass. The bonding procedure was required to form an irreversible bond between the surface of the glass and the unetched portions of the wafer as shown in figure . Anodic bonding was found to provide the simplest means to fulfill the stated requirements.

A description of the anodic bonding process is provided by Terry[12] in 1975: "At elevated temperatures (yet below the 700 C softening point of the pyrex), the positive sodium ions in the glass become quite mobile. They are attracted to the negative electrode on the glass surface where they are neutralized. The more permanently bound negative ions in the glass are left, forming a space charge layer in the glass adjacent to the silicon surface. The time-varying potential distribution is shown in Fig.3.5 (Fig. A1.2 of Terry's text) as a function of position in the glass plate. After the Na^+ have drifted toward the cathode, most of the potential drop in the glass occurs at the surface next to the silicon. The two wafers (the glass and the silicon) then act as a parallel plate capacitor with most of the 600V potential being dropped across the several micron wide air gap between them. The resulting high E-field between the surfaces serves to pull them into contact with a force of 25 Kg/sq. cm. Once the wafers are in contact, almost all of the 600 V potential is dropped across the space charge layer in the glass. The extremely high fields which develop in that region transport oxygen out of the glass to bond with silicon surface. The seal appears to be chemical in nature, similar to a fusion bond, except that the temperatures necessary for silicon-glass fusion are never reached."

The bonding procedure is simple and can be carried out in just a few minutes. The materials are simply stacked in the following arrangement: anode, etched silicon wafer, glass plate, cathode. The entire arrangement is placed on a hot plate. Care must be taken to ensure that the drilled inlet and outlet ports in the glass plate match with the etched inlet and outlet ports in the wafer. (A schematic of the bonding process is included as Fig.3.6.) The hot plate is then heated to 200 C to 400 C and a 600V potential is applied to the electrodes. Heating to a temperature below 200 C may result in incomplete bonding while temperatures above 400 C are dangerous and entirely unnecessary for a complete bond. By cutting a window in the cathode, the bonding may be observed as a gradual change in color of the wafer. Unbonded regions appear light gray while bonded regions appear black. When all raised portions of the wafer appear black, the bonding is complete.

The recommended glass is Corning Pyrex (Code No. 7740). Pyrex is ideally suited to the above described procedure because its coefficient of linear thermal expansion ($3.25 \times 10^{-6}/\text{C}$) is very close to that of silicon ($2.56 \times 10^{-6}/\text{C}$) and it is inexpensive and readily available.

3.5 Final construction

After the anodic bonding is complete, the micromodel consists of a flat glass plate bonded to a flat silicon wafer with an isolated flow path sandwiched between. Short sections of tubing with swagelok end pieces are affixed to the predrilled holes to provide inlet and outlet ports for the model. A high strength epoxy should be used since the contact area for the ports are quite small. The final remaining problem to deal with is the strength of the micromodel. As pointed out in the Anodic bonding section, the bond strength of the silicon to the glass is great, but the strength of the silicon itself is not so great so large pressure drops can cause breakage of the silicon wafer coincident with pore spaces. To strengthen the micromodel, a second glass plate is placed beneath the silicon wafer and the entire stack is epoxied leaving the top epoxy free (Fig.3.7). The resulting micromodels are extremely strong. The micromodels used in this study were pressure tested up to 100 psi before rupture occurred.

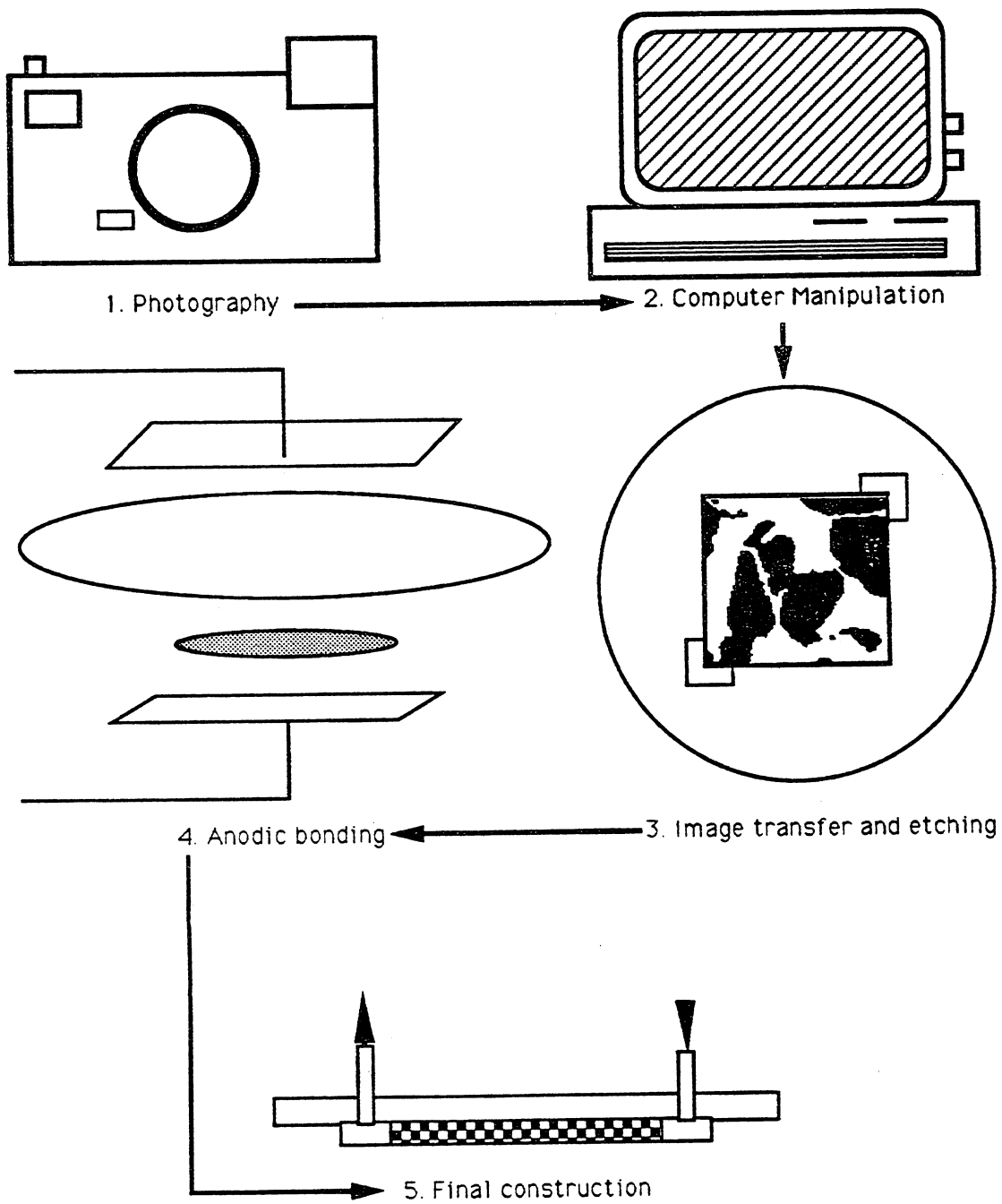


Figure 3.1: Schematic of micromodel construction procedure

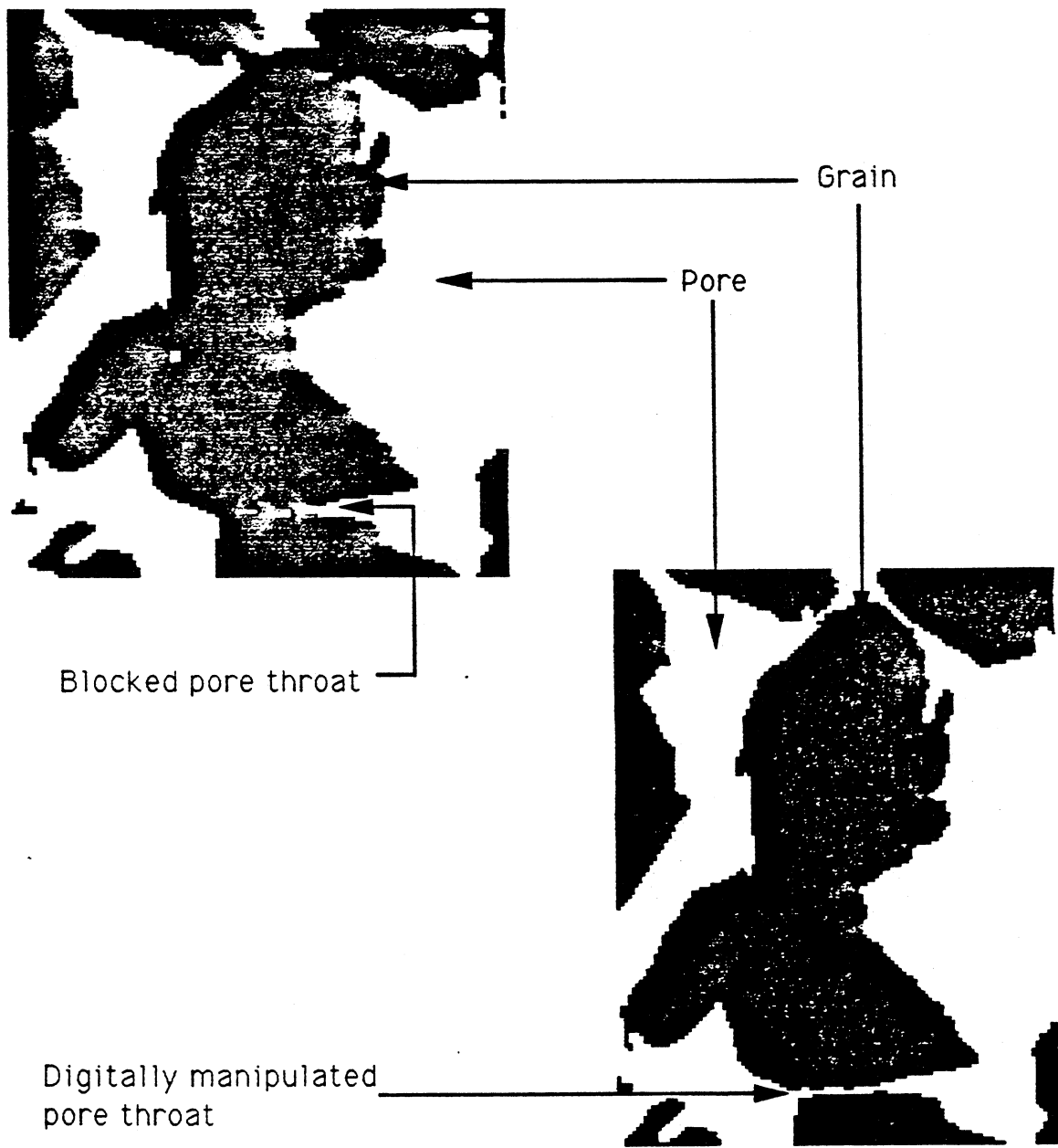


Figure 3.2: Example of digital manipulation

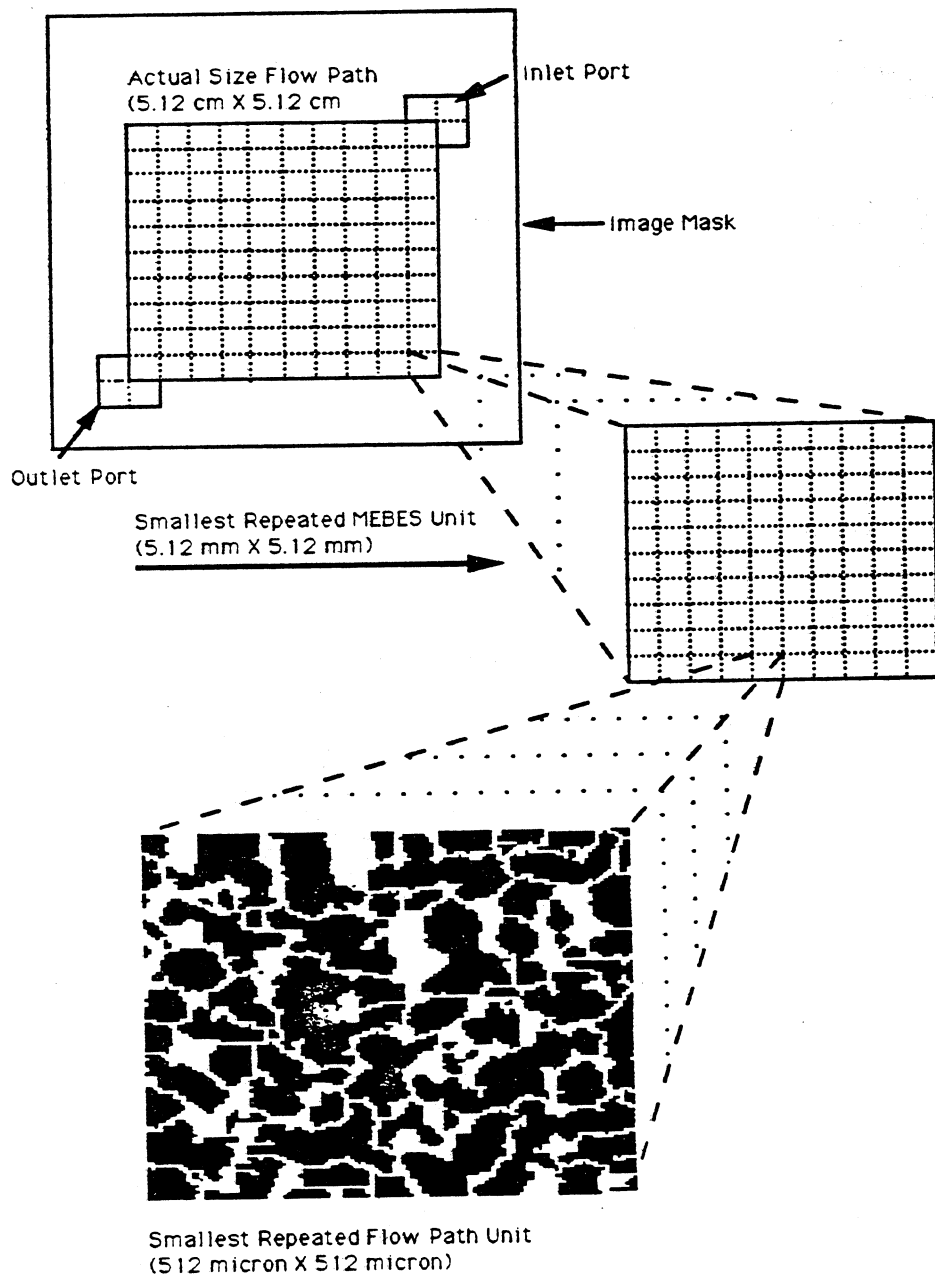


Figure 3.3: Image mask schematic

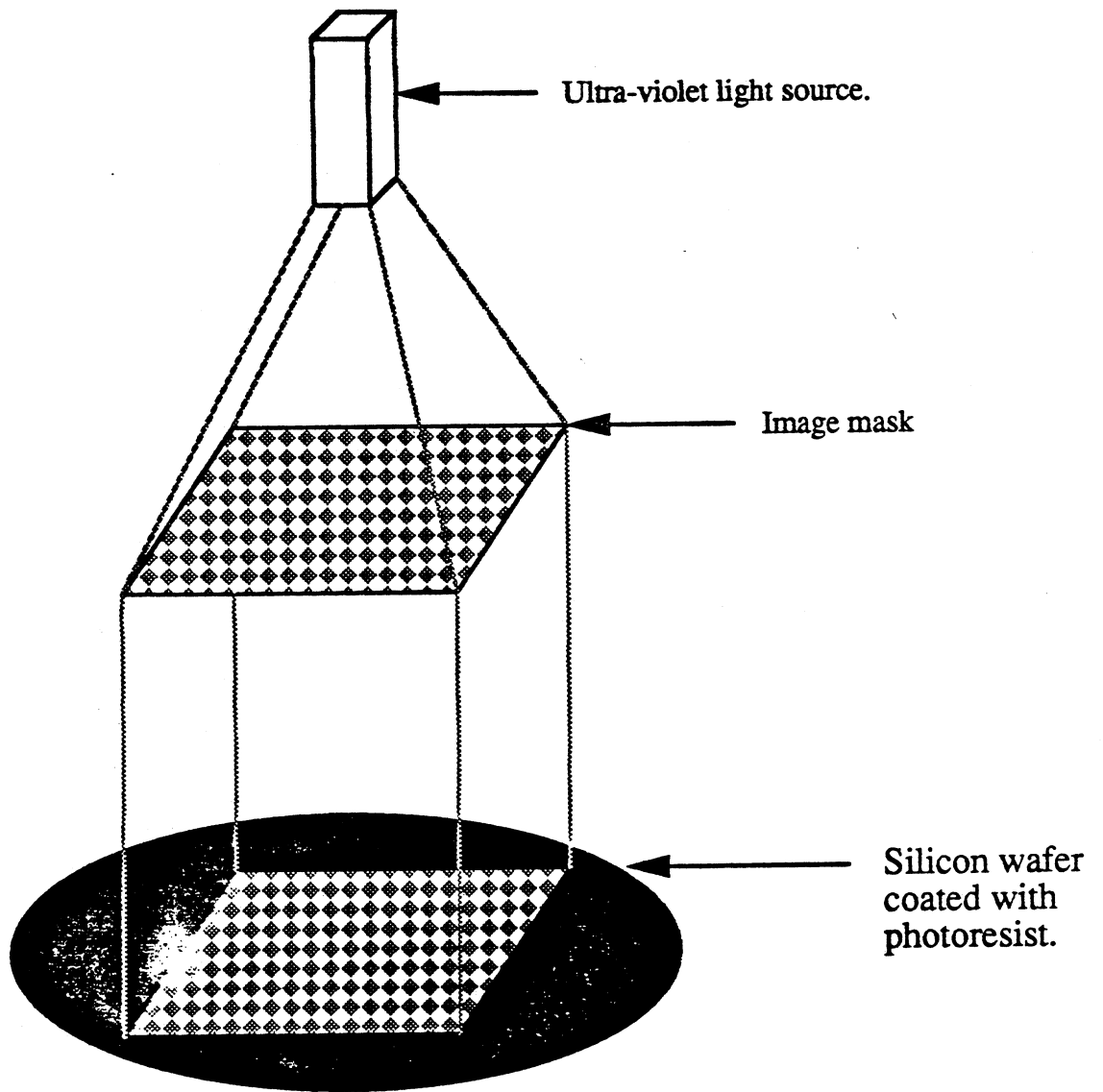


Figure 3.4: Image transfer schematic

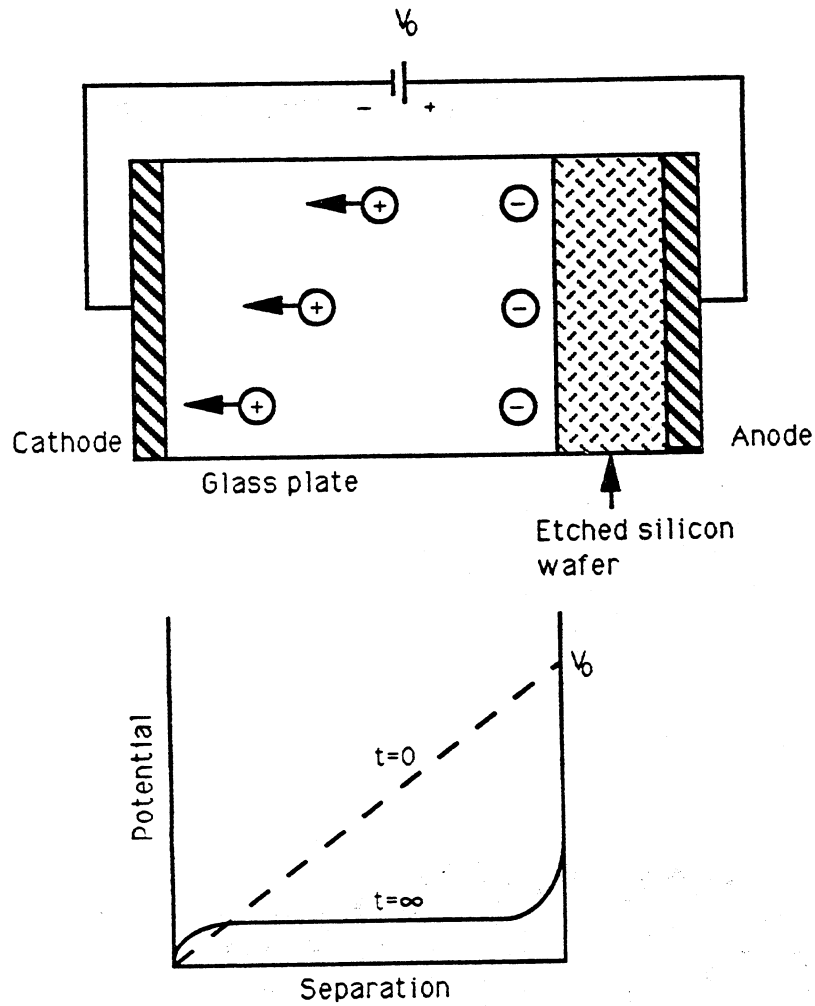


Figure 3.5: Initial and final equilibrium DC potential distributions across the corning glass during anodic bonding. (After Terry)

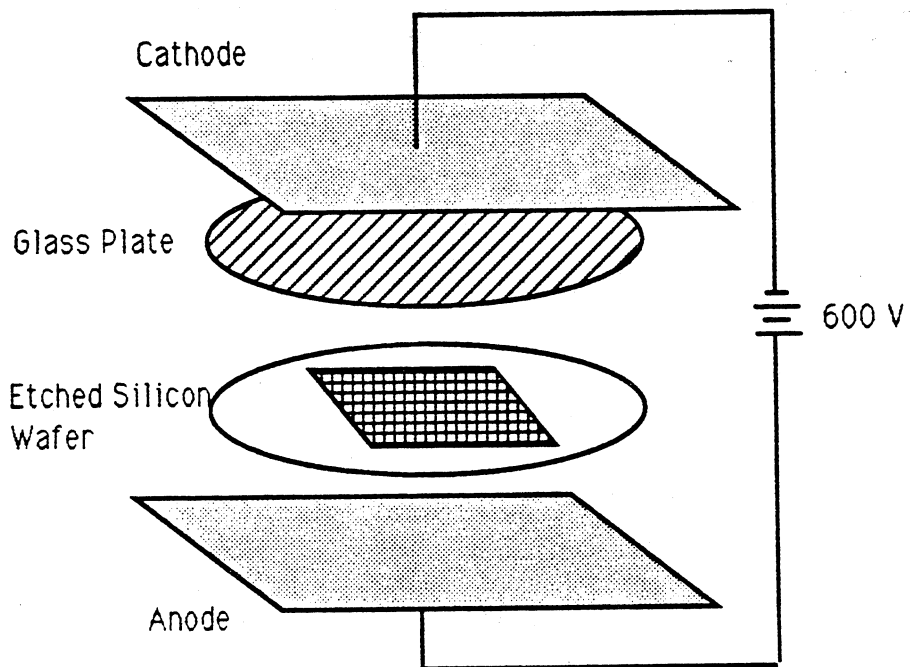


Figure 3.6: Anodic bonding of glass and silicon

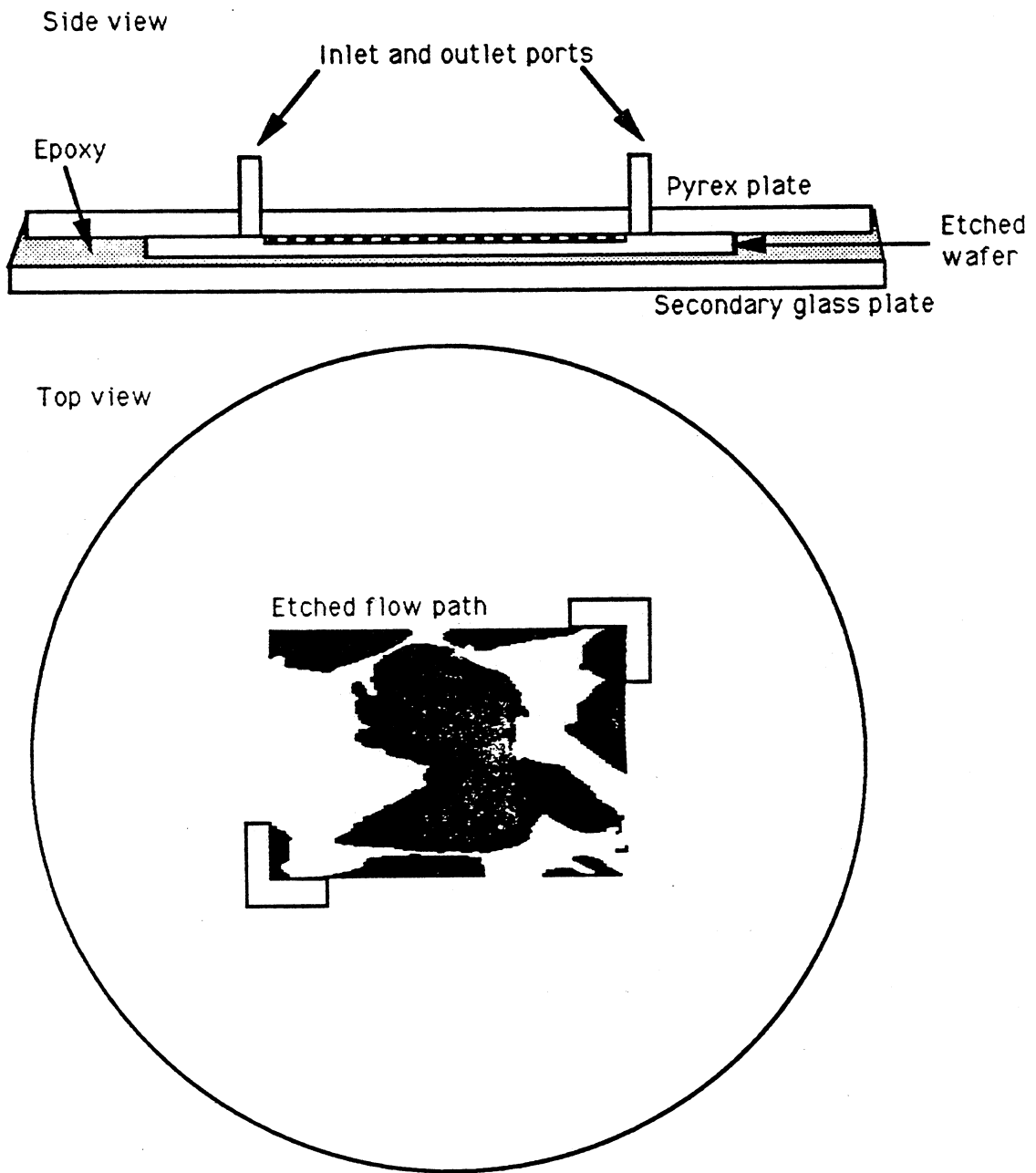


Figure 3.7: Top and side views of completed micromodel

4. Experimental Equipment

In addition to the high resolution micromodels, an experimental apparatus was constructed to enable observation of flow through the micromodels. Figure 4.1 is a schematic of the flow visualization apparatus. It consists of a microscope, still and video cameras, and a high pressure nitrogen tank to create a pressure drop and flow through the micromodels. The microscope used was a Zeiss Axioskop with the capability of magnifying images up to 400 times which is sufficient for the study of pore level events in most porous media. The microscope used had plane light, CID, and ultraviolet light capability. The ultraviolet light capability was necessary for viewing the interface between the oil and the displacing phase due to similarities in color under a conventional light source. The microscope utilized special objectives to increase the depth of the viewing field. Increasing the depth of field was necessary due to the thickness glass plate covering the micromodel. A 3 in. by 5 in. polaroid still camera and a black and white video camera were used to capture flow events seen through the microscope. The video camera was connected to a four-head VHS video recorder and then to a black and white monitor.

The flow system was quite simple for the experiments carried out in this study. Fluids of interests were introduced into the micromodel under vacuum and then flow through the micromodel was induced by use of a high pressure nitrogen tank. Due to the low permeability of the micromodel, flow rates of about one foot per day were achieved but at high pressure drops of 50 psi over the micromodel.

A list of materials used in the experimental procedure is as follows:

1. **Micromodel.** A nearly exact two-dimensional replica of a Berea sandstone was used for all experiments. A description of the micromodel and its construction procedure are detailed in section 3. The smallest pore throat in the micromodel was 1 micron. Porosity of the model was approximately 35 percent. Permeability was not measured exactly but was on the order of a microdarcy.
2. **Microscope.** A Zeiss Axioskop with magnification of 50 to 400 times was used to visualize the pore level events in the micromodel. The microscope was equipped with a 3x5 inch polaroid still camera and a black and white video camera. The microscope had plane, CID, and ultraviolet light capability. Ultraviolet light is absolutely necessary for experiments of the type detailed in this report to distinguish between fluids that appear the same under other types of light.
3. **Driving Mechanism.** The driving force for the flow experiments was a high pressure nitrogen tank. In the slug surfactant experiments, a large reservoir of surfactant was placed between the micromodel and the nitrogen source to assure that no nitrogen would reach the model and create a foam. In foam displacement experiments, a very small amount of surfactant was used to assure that nitrogen would enter the model and generate a foam.
4. **Fluids.** Two fluids were used in the research described in this report. A surfactant filtered to 0.5 micron (AOS 1618) was used as the displacement phase either in slug form or as a foam with nitrogen. The concentration of the surfactant solution was 0.5% the displaced fluid.

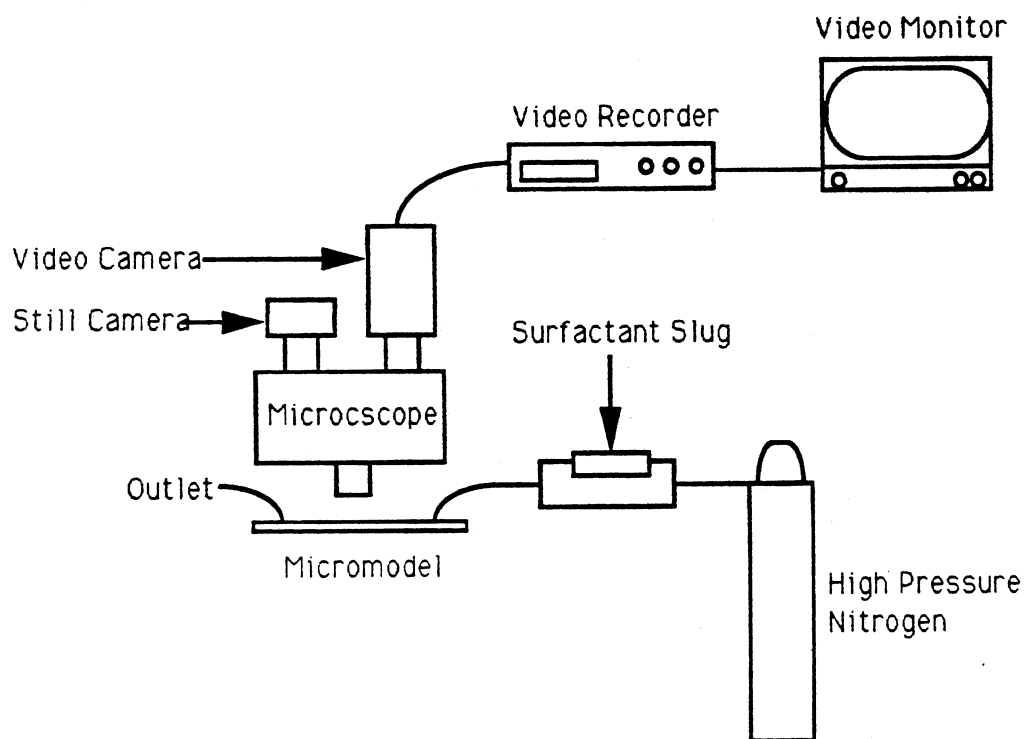


Figure 4.1: Experimental apparatus schematic

5. Experimental Procedure

The effects of oil on foam displacement efficiency were studied qualitatively by observing the oil/displacing phase interface under two different injection schemes. For both displacement schemes, the micromodel was partially filled with oil. In the first case, a slug of surfactant was injected and was allowed to contact and displace the oil bank. In the second case, foam formed in-situ was allowed to contact and displace the oil bank. For both cases, the oil interface was studied to determine any differences between the two displacement schemes. Flow rates for both cases were approximately one foot per day which is a characteristic reservoir flow rate.

5.1 Experimental procedure

Partial saturation of the micromodel with crude oil was accomplished by pulling a vacuum on the micromodel and then opening the micromodel to a container filled with filtered oil. The vacuum was broken when the model was approximately half full so the boundary of the oil bank could be clearly observed. Displacing fluid was introduced into the port not saturated with oil and was driven by a high pressure nitrogen tank. The oil bank boundary was observed and photographed as the displacing phase contacted it. Photography was carried out under ultraviolet light because under plane and CID light, the displacing and displaced phases appeared identical. Differences in the interface under the two different schemes were noted and conclusions were drawn.

5.2 Slug surfactant displacement of oil

In the slug injection scheme, surfactant (AOS 1618) was injected under vacuum and upon contacting the oil, the oil/surfactant interface was observed. Under this displacement scheme, the oil appeared to be the wetting phase. It occupied the small pores and lined the surfaces of the grains while the surfactant occupied the large pores (Fig.5.1). In the figure cited, the surfactant appears dark while the oil appears light due to the filter used. Since the oil phase fluoresces much brighter, and since most of the image is either rock or surfactant, low light photography was used in order to make the interfaces as clear as possible. The use of low light photography has eliminated some of the detail that may be seen by the naked eye, but enough detail is preserved that the oil is clearly seen to be the wetting phase while the surfactant is observed to be the non-wetting phase by virtue of its existence as distinct blobs. Apparently, the crude had sufficiently altered the wettability of the silicon micromodel in a very short time (by deposition of polar components in the crude oil) to create an oil wet system. Displacement of oil under these conditions should yield a fairly efficient displacement as all the oil in the large pores is displaced leaving only the oil in the smaller pores behind. That displacement of oil by a slug of surfactant followed by foam is an efficient means of oil displacement is consistent with earlier research, specifically that reported by Hutchinson (Section 2).

5.3 Foam displacement of oil

For the foam displacement scheme, a small amount of surfactant was injected under vacuum in the port not containing oil and then was displaced toward the oil bank by high pressure nitrogen. The gas was observed to move through the surfactant slug generating first bulk foam and, later on, a high quality foam (Figs.5.2 and 5.3). An idea of the foam quality can be obtained by observing

the number of lamellae per pore. The bulk foam contains many lamellae in each pore while the high quality foam may have only one lamella in each pore. Photography of the foam propagating in the porous medium was straight-forward. Since only one phase was present, light levels were easy to control and, as a result, highly detailed photographs were possible.

The foam, formed in-situ, eventually contacted the oil bank and the interface was observed. Most of the lamellae were destroyed upon contact with the oil bank and, in this injection scheme, the surfactant appeared to be the wetting phase. It occupied the small pores and coated the grains (Fig.5.4). In the cited figure, the oil phase appears as the dark blobs while the thin surfactant films appear white. The contrast in this image has been enhanced by thresholding techniques. In the actual photograph, there was such small contrast between the oil and surfactant phases that they were almost indistinguishable. As a result, it was necessary to alter both the contrast between the phases and the entire gray scaling of the image. The result, however, closely replicates the image that may be seen with the naked eye and preserves the important details of the displacement process. That the liquid portion of the foam becomes the wetting phase under the foam displacement scheme is in agreement with results of Sanchez and Hazlett (Section 2) who found that foam injection into an oil wet porous medium alters the wettability of the surfaces.

Since the surfactant is, under this displacement scheme, the wetting phase, the displacement front would not be expected to be a stable one and fingers would be expected to develop easily. The surfactant, under this scheme, would tend to travel along grains and break through at the production port before a significant amount of oil has been produced. Again, the expected displacement efficiency, based upon the observed displacement front, is consistent with previous research, especially that reported by Hutchinson.

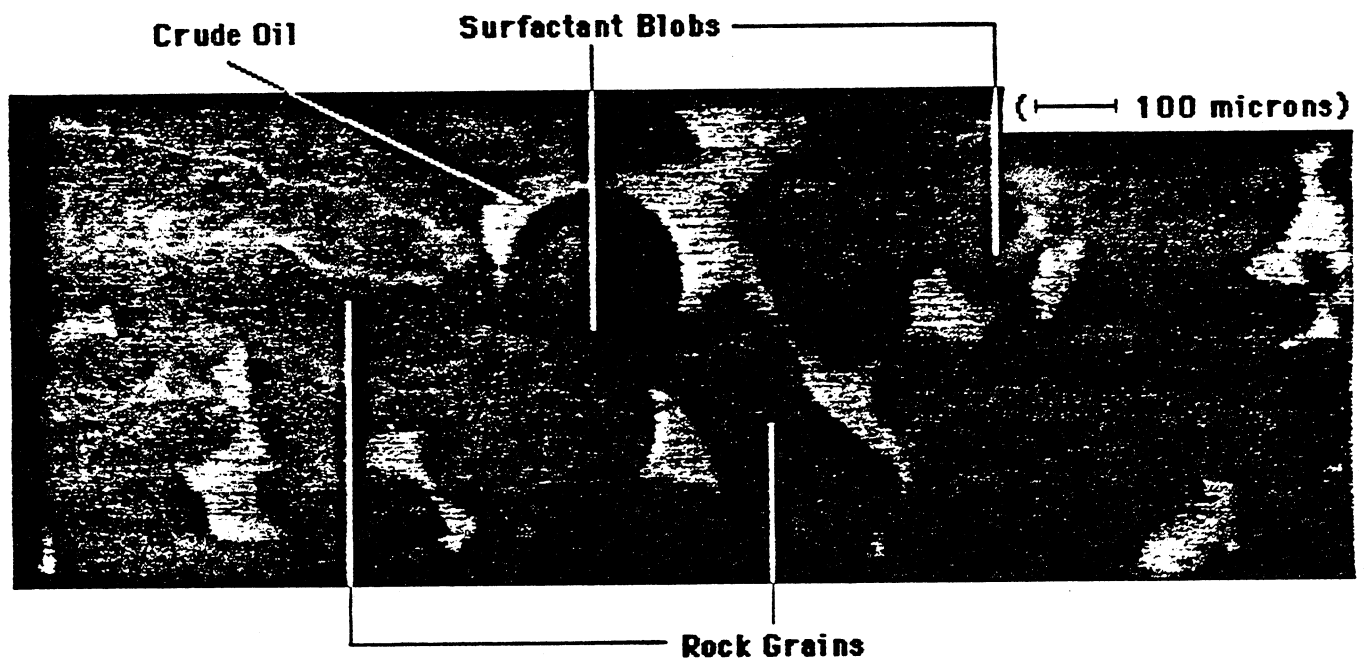


Figure 5.1: Crude oil/slug-surfactant interface

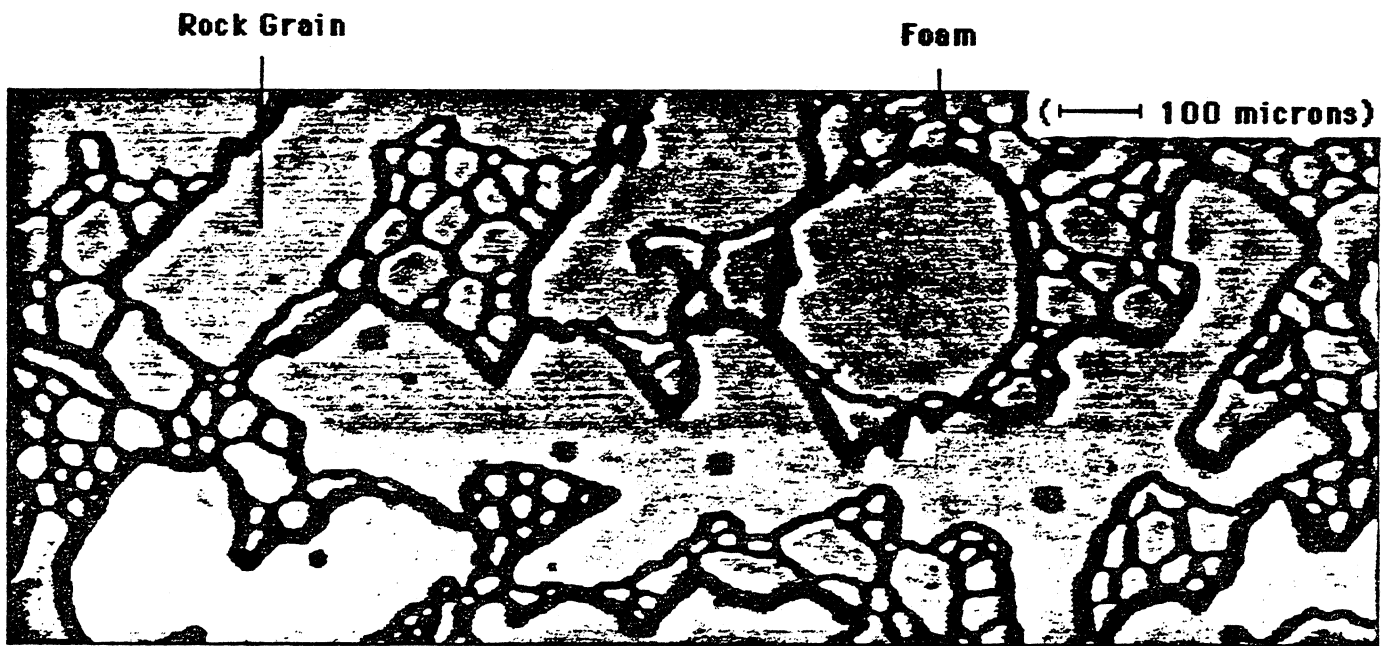


Figure 5.2: Bulk foam near injection port - far from oil bank

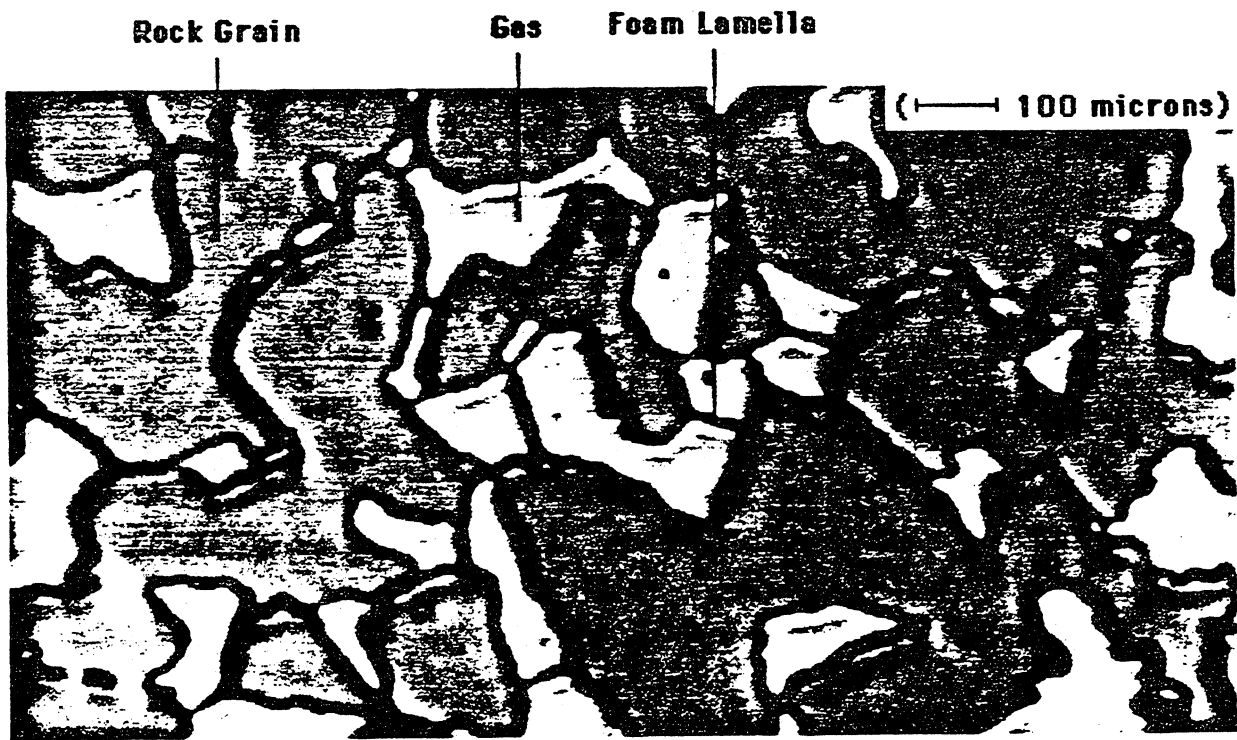


Figure 5.3: High quality foam in porous medium

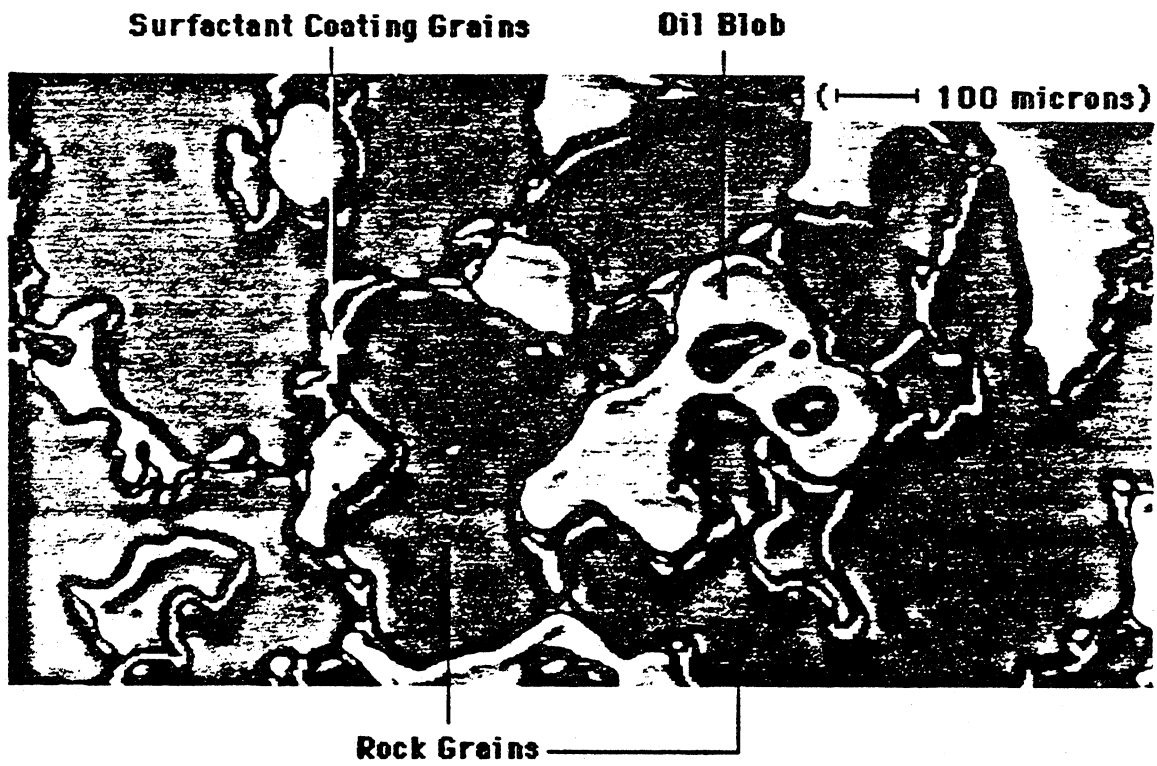


Figure 5.4: Crude oil/foam interface

6. Conclusions

Conclusions provide insights into the mechanisms by which oil is displaced from porous media by foams and also indicate that more research in high resolution micromodels may be helpful in understanding oil displacement mechanisms:

1. A high resolution, two-dimensional, sandstone replica micromodel has been constructed to be used as a tool to observe pore level events in flow through porous media. The technology developed allows for construction of a replica of any type of porous medium that may be of interest to researchers. Experiments in which the displacement of crude oil by surfactant slug and by foam were observed indicate the usefulness of the new micromodels.
2. The injection procedure used in displacing oil with foam has been shown to strongly influence the efficiency of the oil displacement. Fundamental differences in the oil/displacement phase interface were observed when slug surfactant or foam was used to displace the oil in a porous medium of intermediate wettability.
3. When slug injection of surfactant was used to displace the oil, an efficient displacement was achieved. Polar components in the oil had sufficiently altered the surface of the porous medium to make it oil wet. The displacing surfactant was observed to push the oil from the large pores resulting in a large fractional displacement of oil before surfactant breakthrough.
4. When foam formed external to the oil bank was used to displace the oil, a very inefficient displacement was achieved. The foam was observed to break upon contact with the oil phase and the liquid portion of the foam was observed to wet the porous medium. Due to channeling of the surfactant along the grains in the porous medium, displacement of oil by externally generated foam would be expected to lead to early breakthrough of surfactant with very low fractional recovery of oil. This behavior as well as the observed behavior of oil displacement by slug injection of surfactant may provide an explanation for the phenomena reported by Hutchinson. The mechanism by which surfactant becomes the wetting phase in a porous medium of intermediate wettability in the presence of crude oil when a foam is the displacing phase is described by Sanchez and Hazlett (Section 2). However, more research in this area should yield interesting and important results pertaining to the displacement of oil by foams.

7. Recommendations

The research detailed in this report and summarized in the "Conclusions" section was carried out to construct a new micromodel for study of pore level events and, using that micromodel, to gain insight into the effects of oil on foam under different oil displacement schemes. While a new, high resolution micromodel was constructed and important insights were gained into oil displacement by foam, there are improvements that may be made to the micromodel itself and much additional research that should be carried out to better understand the displacement of oil by foams. Some improvements to the research outlined in this report and recommendations for future research are as follows:

1. To increase the permeability of the micromodels, the etch depth in models built in the future should be around 30 microns instead of the 5 micron depth used in current micromodels. In order to increase the etch depth, the smallest pore throat may have to be increased from the 1 micron currently used to 2 or 3 microns but this is still on the correct order of magnitude for a real porous medium.
2. Future research should consider foams created by several different surfactants, and at several different concentrations. The research outlined in this report used only one surfactant at one concentration. To better understand the fundamentals of the foam displacement of oil, as wide a range as possible of surfactant types and concentrations should be used.
3. Future research should investigate the displacement characteristics of surfactants on several oils. The research in this report considers only a single crude oil. A better understanding of the effects of oil on foam stability would be achieved by using a range of oils from light, refined oils to heavy crudes.
4. Future research should more fully investigate the effects of wettability on foam stability. In this report, wettability was not a major focus area. Only a high energy surface (Silicon dioxide) was used with no special surface preparation. By preparing the micromodel surfaces to create a range of specific wettabilities, more insight into the effects of wettability on foam stability should be achieved.

Appendix A. Computer Program

```
/*
 * tiff2cif - Program to convert binary tiff file to cif format
 *
 * David Ashkenas 14 Dec 90
 *
 * File is assumed to be organized as follows:
 * Header is 246 bytes long, as described below (struct header).
 * Data is organized in rows, starting with the top row.
 *
 * Command line arguments:
 * tiff2cif <filename> [<minboxwidth>] [-blt]
 * where <filename> is tiff file name
 * <minboxwidth> is optional small box filter; boxes smaller
 * than this will not be output; default is 2 um
 * -blt causes blt instead of cif to be produced.
 *
 * Pixel size of tiff input is fixed at 1um x 1um.
 * Produces cif (default) or blt on stdout.
 *
 */
```

```
#include <stdio.h>
#include <sys/file.h>
```

```
/* header record: 246 bytes */
struct header { short magic ; /* magic number; see below */
short unused1[14] ;
short numcols ;
short unused2[5] ;
short numRows ;
short unused3[59] ;
int filesize ;
short unused4[40] ;
} tiffhead ;
```

```
#define MagicNum 0x4d4d
```

```
char bitrow[700] ;
int docif = 1 ;
int minboxwidth = 2 ;
```

```
main ( argc, argv )
int argc ;
char **argv ;
```

```

{
char *filename ;
int tfd ;
int i ;
int bytesperrow ;
int status ;
int rasternum = 0 ;

if ( argc < 2 ) {
    fprintf ( stderr, "Usage: tiff2cif <file> [<minboxwidth>] [-blt]\n" ) ;
    exit ( 1 ) ;
}
tfd = open ( filename = argv[1], O_RDONLY ) ;
if ( tfd == -1 )
    fatalerr ( "File open error: %s", argv[1] ) ;

/* Pick up optional command line arguments; they can be in any order */
if ( argc > 2 ) {
    for ( i = 2 ; i < argc ; i++ ) {
        if ( strcmp ( argv[i], "-blt" ) == 0 )
            docif = 0 ;
        else if ( 1 == sscanf ( argv[i], "%d", &minboxwidth ) ) {
            if ( minboxwidth < 1 )
                minboxwidth = 2 ;
        }
    }
}
doheader ( filename ) ; /* Write output file header */
read ( tfd, &tiffhead, sizeof ( tiffhead ) ) ;
if ( tiffhead.magic != MagicNum )
    fatalerr ( "Wrong input file format (bad magic number)" ) ;
if ( tiffhead.numcols == 0 || tiffhead.numrows == 0 )
    fatalerr ( "Wrong input file format (bad row/column count)" ) ;

bytesperrow = ( tiffhead.numcols + 7 ) / 8 ; /* ceiling ( cols / 8 ) */
for ( i = 0 ; i < tiffhead.numrows ; i++ ) {
    status = read ( tfd, bitrow, bytesperrow ) ;
    if ( status == -1 )
        fatalerr ( "file read error" ) ;
    else if ( status == 0 )
        fatalerr ( "unexpected EOF" ) ;
    else if ( status != bytesperrow )
        fatalerr ( "expected to read %d bytes; got %d", bytesperrow, status ) ;

    rasternum++ ;
    ras2boxes ( tiffhead.numcols - rasternum ) ; /* Convert raster to boxes */
} /* end for loop */

```

```

dotrailer ( ) ; /* Do rest of cif file stuff */
close ( tfd ) ;
exit ( 0 ) ;
}

doheader ( fname )
char *fname ;

/* Write cif or blt header to stdout.
 * Note on cif scaling: input pixels are assumed to be 1 um square.
 * To represent the center of any box, need 1/2 um resolution.
 */
{
if ( docif ) {
printf ( "DS 1 50 1;\n" ) ;
printf ( "9 %s;\n", fname ) ;
printf ( "L M1;\n" ) ;
}
else {
printf ( @"\@\\(\#\\) %s\n", fname ) ;
printf ( "unit 1um\n" ) ;
}
}

dotrailer ( )
/* Write cif or blt trailer to stdout */
{
if ( docif ) {
printf ( "DF;\n" ) ;
printf ( "C 1;\n" ) ;
printf ( "End\n" ) ;
}
}

ras2boxes ( ycoord )
int ycoord ;

/* Convert a single raster from bit image to boxes.
 * Raster is contained in the global array bitrow[]. */
{
int j, k ;
int thisdigit ;
int bytesperrow ;
int xstart, xstop ;
int doingbox ;

bytesperrow = ( tiffhead.numcols + 7 ) / 8 ;

```

```

doingbox = 0 ;
for ( j = 0 ; j < bytesperrow ; j++ ) {
    thisdigit = bitrow[j] ;
    if ( thisdigit != 0 ) {
        /* this byte contains one or more pixels */
        for ( k = 0 ; k < 8 ; k++ ) {
if ( thisdigit & ( 128 >> k ) ) {
    /* this bit is on */
    if ( ! doingbox ) {
        doingbox = 1 ; /* start of a rectangle */
        xstart = ( j << 3 ) + k ;
    }
}
else {
    /* this bit is off */
    if ( doingbox ) {
        doingbox = 0 ;
        xstop = ( j << 3 ) + k ;
        dumpbox ( xstart, ycoord, xstop, ycoord+1 ) ;
    }
}
        } /* end for k: each bit in byte */
    } /* end if: this byte was non-zero */
    else {
        /* this byte is zero; check for end of rectangle */
        if ( doingbox ) {
doingbox = 0 ;
xstop = j << 3 ;
dumpbox ( xstart, ycoord, xstop, ycoord+1 ) ;
        }
    }
} /* end for j: each character in raster[] */
}

```

```

dumpbox ( x1, y1, x2, y2 )
    int x1, y1, x2, y2 ;

```

```

/* Dump box dimensions to stdout in either cif or blt format */

```

```

{
if ( ( x2 - x1 ) >= minboxwidth ) {
    if ( docif )
        printf ( " B %d %d %d %d;\n",
            ( x2 - x1 ) * 2, /* length */
            ( y2 - y1 ) * 2, /* width */
            ( x2 - x1 ) + ( x1 * 2 ), /* x center */
            ( y2 - y1 ) + ( y1 * 2 ) ) ; /* y center */
}
}

```

```
    else
        printf ( "box %d %d %d %d\n", x1, y1, x2, y2 ) ;
    }
}
```

```
fatalerr ( msg, p1, p2 )
{
    fprintf ( stderr, msg, p1, p2 ) ;
    fprintf ( stderr, "\n" ) ;
    exit ( 1 ) ;
}
```

References

- [1] Bond, D. C. and Holbrook, O. C.: "Gas Drive Oil Recovery Process," U.S. Patent No. 2,866,507 (1958).
- [2] Huh, D. G. and Cochrane, T. D.: "The Effect of Microscopic Heterogeneity on CO₂-Foam Mobility," *JPT* (1989) 41, No. 8, 872-879.
- [3] Hutchinson, D. A.: "Steam Foam Studies in the Presence of Residual Oil," SUPRI Annual Report No. TR-80, Stanford University (1990).
- [4] Jimenez, A. I. and Radke, C. J.: "Dynamic Stability of Foam Lamellae Flowing Through a Periodically Constricting Pore," Symposium on Advances in Oil Field Chem. Third Chem. Cong. of the North American Continent and 195th National Meeting of ACS, Toronto, Canada (1988).
- [5] Manlowe, D. J. and Radke, C. J.: "A Pore-Level Investigation of Foam/Oil Interactions in Porous Media," paper SPE 18069 presented at the 1988 SPE Annual Technical Conference and Exhibition, Houston, oct., 5-8.
- [6] Marsden, S. S.: "Foams in Porous Media," SUPRI Report No. TR-37, Stanford University (1986).
- [7] Marsden, S. S., Elson, T., and Guppy, K.: "Literature Review of the Selective Blockage of Fluids in Thermal Recovery Procedures," SUPRI Report No. TR-3, Stanford University (1977).
- [8] Nikolov, A. D., Wassan, D. T., Huang, D. W., and Edwards, D. A.: "The Effect of Oil on Foam Stability: Mechanisms and Implications for Oil Displacement by Foam in Porous Media," paper SPE 15443 presented at the 1986 SPE Annual Technical Conference and Exhibition, New Orleans, Oct., 5-8.
- [9] Owete, O. S. and Brigham, W. E.: "Flow of Foam Through Porous Media," Contract No. DOE-SF-11564, U.S. DOE (July 1958).
- [10] Sanchez, J. M. and Hazlett, R. D.: "Foam Flow Through an Oil-Wet Porous Medium: A Laboratory Study," paper SPE 19687 presented at the 1989 SPE Annual Technical Conference and Exhibition, San Antonio, Oct., 8-11.
- [11] Sarathi, P.: "Using Micromodels to Study Steam Displacement Processes in Porous Media," Contract No. NIPER-180, U.S. DOE (August 1986).
- [12] Terry, C. S.: "A Gas Chromatography System Fabricated on a Silicon Wafer Using Integrated Circuit Technology," Integrated Circuits Laboratories Technical Report No. SEL-75-011, Stanford University (1975).

